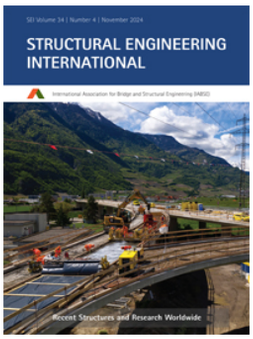

Structural Engineering International

ISSN: (Print) (Online) Journal homepage: www.tandfonline.com/journals/tsei20

Damage-Sensitive Feature for Long-Span Steel Box-Girder Suspension Bridges Under Service Loads Based on Long-Term Monitoring

Yuefeng Shao Dr, Changqing Miao Prof., Zheheng Chen Prof., Mei-Ling Zhuang Dr, Chuanzhi Sun Dr, Hanbo Zhu Dr & Yongsheng Zhang

To cite this article: Yuefeng Shao Dr, Changqing Miao Prof., Zheheng Chen Prof., Mei-Ling Zhuang Dr, Chuanzhi Sun Dr, Hanbo Zhu Dr & Yongsheng Zhang (27 Nov 2024): Damage-Sensitive Feature for Long-Span Steel Box-Girder Suspension Bridges Under Service Loads Based on Long-Term Monitoring, Structural Engineering International, DOI: 10.1080/10168664.2024.2407100

To link to this article: https://doi.org/10.1080/10168664.2024.2407100

Published online: 27 Nov 2024.

Damage-Sensitive Feature for Long-Span Steel Box-Girder Suspension Bridges Under Service Loads Based on Long-Term Monitoring

Yuefeng Shao, Dr, School of Architecture and Civil Engineering, Jiangsu Univ. of Science and Technology, Zhenjiang, People's Republic of China; **Changqing Miao**, Prof., School of Civil Engineering, Southeast University, Nanjing, People's Republic of China; **Zheheng Chen**, Prof., School of Architecture and Civil Engineering, Jiangsu Univ. of Science and Technology, Zhenjiang, People's Republic of China; **Mei-Ling Zhuang**, Dr, Water Resources Research Institute of Shangdong Province, Jinan, People's Republic of China; School of Transportation and Civil Engineering, Nantong University, Nantong, People's Republic of China; **Chuanzhi Sun**, Dr, School of Civil Engineering and Architecture, Suqian College, Suqian, People's Republic of China; **Hanbo Zhu**, Dr, School of Civil Engineering and Architecture, Suqian College, Suqian, People's Republic of China; **Yongsheng Zhang**, Jiangsu Provincial Transportation Engineering Group CO., LTD, 398 Guyang East Rd., Zhenjiang, People's Republic of China.
Contact shyfeng007@just.edu.cn; chqmiao@163.com
DOI: 10.1080/10168664.2024.2407100

Abstract

To extract valuable data from long-term monitoring and identify structural damage to ensure the serviceability and safety of bridges, a commonly used method in large bridge maintenance. This article developed a time-domain energy-based method for identifying bridge damage based on long-term *structural health monitoring* noisy output measurements. This method first calculated an energy threshold within the structural frequency bandwidth of natural vibration at measurement points. Then, the structural damage was assessed by computing the time-domain energy accumulation. The improved procedure of this proposed method involved extracting modal frequencies from the signal for each modal order, determining the structural frequency bandwidth of natural vibration, and applying the square root envelope method to smooth vibration data and mitigate the impact of abnormal signals. Later, the applicability of the proposed method for damage identification was verified by comparing it with conventional modal flexibility and modal curvature methods. Finally, a case study on the Runyang bridge, a supported steel-box-girder suspension bridge with a main span of 1490 m in China, was made for demonstration. The results indicated that the area between 1/4-span and 1/2-span of the bridge was more sensitive to damage under service loads. The method performed well in identifying potential damage locations and assessing vulnerability. The calculation results using the method proposed in this article were consistent with those of traditional methods. The research offers methodological backing for utilizing extensive data monitoring in evaluating structural damage.

Keywords: damage identification; time-domain energy; Structural health monitoring; long-span steel box-girder suspension bridges; long-term monitoring vibration data; modal flexibility; modal curvature.

Introduction

Long-span steel box-girder bridges have been widely used in modern transportation systems because of their advantages, such as aesthetically pleasing design, robust spanning ability, stable quality, and enhanced driving comfort. However, under long-term loads, long-span bridges inevitably experience fatigue damage.[1,2] Existing damage identification methods are predominantly based on numerical simulations and short-term test data,[3] mainly applied to individual components or smaller structures.[4] Long-term structural health monitoring (SHM) is essential to study the damage evolution of actual long-span bridges.

In the past decades, various methods have been proposed to identify structural damage, such as modal parameter-based techniques,[5–7] mode shape-based damage detection method,[8–10] damping-based damage detection method,[11,12] signal processing-based approaches,[13–15] and finite element model updating methods.[16,17] The experimental study[18] shows that the change in stiffness caused by structural damage will be reflected in the structural mode. And the damage cracks will be highly effective in affecting the structure's natural frequencies, corresponding mode shapes, and damping ratios.[19] Thus, the vibration-based damage detection method by modal parameters[20,21] were widely used to assess structural damage. For example, Ref. [22] introduced that the influence of structural damage on structural stiffness can be well reflected in the modal characteristics extracted by the Stochastic Subspace Identification (SSI) methods, and the damage location of the structure can be determined accurately. Reference [23] proposed that structural damage consistently impacts natural frequencies and modal damping predictably. This damage inspection method was validated through experiments on a welded steel frame and wire rope. This study demonstrated the feasibility of using modal parameters to identify structural damage, but the experiments were conducted with a simplified structure and idealized loads. Reference [24] employed an artificial neural network to denoise the original data. They assessed steel beams' damage under impulse input excitation using modal flexibility, strain energy, and modal curvature. The approach successfully identified the damage location of the steel beam. However, the excitation of long-span bridges to obtain modal parameters or signals is usually labor-intensive and costly. It

also affects the regular traffic on the bridges. There are also some problems in numerical simulations for damage identification of long-span bridges, such as the discrepancy between analytical results and actual conditions due to the complexity of actual loads and the considerable computational demands.

The development and maturity of SHM technology offer the possibility of monitoring large-scale structures' long-term, real-time health statuses.[25] Combining structural damage identification methods and the output data of SHM systems to conduct long-term structural damage-sensitivity feature analysis on large structures makes it possible to effectively reduce human and material resources while maintaining an appropriate amount of calculations. This also makes it possible to use damage identification methods to conduct real-time assessments of damage-sensitive features of structures. Reference [26] investigated damage identification methods based on the measured data from the SHM system and deemed that abnormal data, ambient noise, and inappropriate processing can lead to unsatisfactory results in damage identification. With the widespread use of long-span bridges, applying SHM systems to assess structural conditions is becoming increasingly common.

This article developed a time-domain energy-based method for analyzing the damage-sensitive feature for the bridges based on long-term SHM output measurements to more effectively use the bridge health monitoring system to determine its health status. The research outline is as follows: Section 2 presents the theoretical framework for the damage-sensitive feature assessment and verification approach. Section 3 presents detailed information on the SHM system of Runyang Bridge, along with its modal parameters. Section 4 gives the damage-sensitive feature analysis and corresponding verification process using monitoring data from 2008 and 2014.

Damage-Sensitive Feature Assessment Method

Improved Energy-Based Damage-Sensitive Feature Assessment

Vibration-based damage identification methods that examine the changes in a structure's global vibration characteristics were regarded as global methods that had attracted much attention in the past decades.[27] Accelerations have been used to identify bridge damage in bridge SHM systems. However, bridge damage identification was an optimization challenge because it involved highly uncertain monitoring parameters influenced by environmental factors.

To reduce the impact of environmental factors, a band-pass filtering of the acceleration time history was performed to extract the natural vibration signal of the bridge. The cut-off frequency and bandwidth of the filtering were determined based on the natural frequencies of the bridge. Additionally, a root-mean-square (RMS) envelope was applied to mitigate the effects of distorted signals, producing a more easily analyzable waveform. A comparison of the acceleration time history at the mid-span of the bridge girder with the RMS envelope was shown in *Fig. 1*. By retaining the trend in the acceleration amplitude, the envelope diagram effectively filtered out data with drastic amplitude changes, simplifying the analysis of the acceleration time history waveform.

Considering $y(t_k)$ as the authentic output vectors of a structure at the time instant t_k, $k = 1, 2, \ldots, n_{\text{time}}$, the RMS envelope of the signal can be written as:

$$\begin{bmatrix} y_{up}(t_k) & y_{low}(t_k) \end{bmatrix} = f_{RMS}\begin{bmatrix} y(t_k), & w \end{bmatrix} \quad (1)$$

where n_{time} is the number of sampling points within the recorded time histories; $y_{up}(t_k)$ and $y_{low}(t_k)$ are the upper and lower RMS envelopes of the output vectors, respectively; w signifies the length of the sliding window within the RMS envelope.

The bridge natural vibration signal and RMS envelope signal are described in *Fig. 1*. The envelope diagram filtered out sharp amplitude data and retained the amplitude variation trend of the acceleration. This procedure leaded to a relatively smoother waveform, thereby mitigating the impact of abnormal data points on the analysis. Setting the sliding window length w to 150 can obtain a smoother envelope without changing the temporal evolution trend.

Damage-induced decrease in structural stiffness led to time-domain energy fluctuations in the signal. The acceleration time-history curve's upper and lower envelope curves were used to compute the time-domain energy associated with acceleration vibration within the time interval Δt. The improved time-domain energy can be expressed as:

$$E_{RMS} = \sum_{j=1}^{n_{rec}} \sum_{k=1}^{n_{time}} \left(y_{up}^{j}(t_k + \Delta t) - y_{low}^{j}(t_k + \Delta t)\right)^2 \times \Delta t,\ k = 1, 2, \ldots, n_{time} \quad (2)$$

where n_{rec} is the count of recorded time histories, a value contingent upon the amount of monitoring data.

The goal of bridge damage identification was to confirm the location

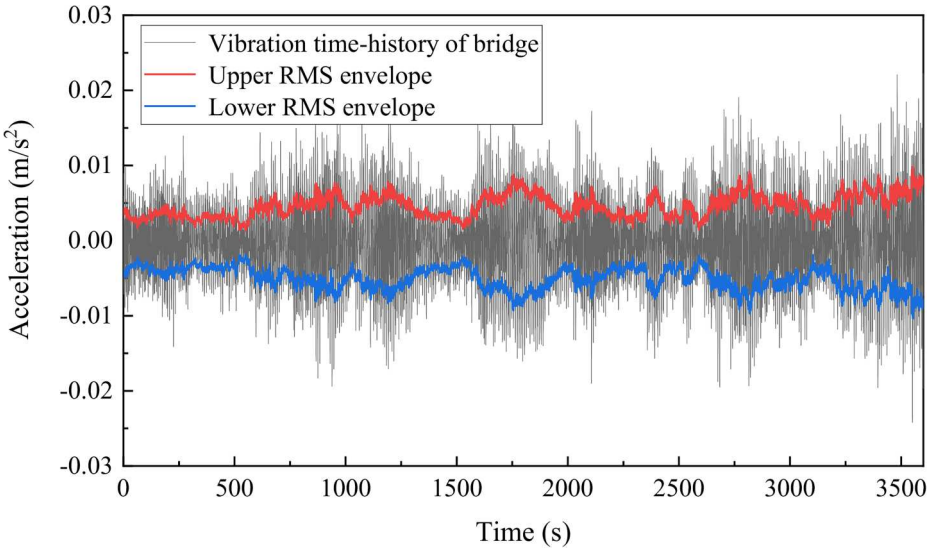

Fig. 1: Bridge natural vibration signal and RMS envelope signal

and severity of potential damage by contrasting the bridge damage indicators at different stages of measurement points. Considering the acceleration time history acquired by bridge SHM system, the relative alteration of time-domain energy E can be regarded as the damage parameter H. Then, the damage conditions of the structure can be assessed by the proportion of damage parameter H at each measurement point. The equations for this procedure can be written as:

$$H_j = |E_{op} - E_{or}|/E_{or} \tag{3}$$

$$Q_j = |H_j|/\sum_{j=1}^{n_s} |H_j|, j = 1, 2, \ldots, n_s \tag{4}$$

$$T_j = \left| Q_j - \frac{\sum_{j=1}^{n_s} Q_j}{n_s} \right| \tag{5}$$

where E_{op} is the time-domain energy of the bridge's acceleration time history during operation; E_{or} is the time-domain energy of the acceleration time history in the initial state of the bridge; Q_j is the proportion value of the H at the jth measuring point relative to the sum of H over all the measurement points; T_j is the threshold employed for the assessment of the structural state at the jth measurement point; and n_s is the count of accelerometers within the health monitoring system.

For a comprehensive quantitative analysis of the structural state, the H value was normalized using Eq.(4). According to Eq.(5), the threshold value T_j for structural state assessment was calculated for the structural location at the jth measurement point. Then, the threshold value T_j and the mean value $(\sum Q_j)/n_s$were compared. If T_j exceeded $(\sum Q_j)/n_s$, it stated that structural damage may exist at the jth measuring point, and the value indicated the relative degree of damage.

Modal Parameter-Based Damage-Sensitive Feature Assessment

In traditional vibration-based damage detection techniques, structural damage can be reflected by changes in the dynamic properties of the structure, including mode shapes, modal damping, and natural frequencies.[28,29] These methodologies relied on the characteristics derived from the dynamic parameters, They were classified into several categories: mode shape-based methods, natural frequency-based methods, strain curvature mode shape-based methods, and alternative modal parameter-based methods.[24,30,31] This article uses the structural modal flexibility and curvature methods to assess the applicability of the structural damage identification methods in Section 2.1.

Modal Flexibility Method

The structural identification index at jth measuring point based on modal flexibility[32] change can be defined as:

$$MFDSI_j = \frac{\left[\sum_{i=1}^{n} \left| \frac{1}{\omega_i^2} \phi_{ij}\phi_{ij} \right| \right]_{p2} - \left[\sum_{i=1}^{n} \left| \frac{1}{\omega_i^2} \phi_{ij}\phi_{ij} \right| \right]_{p1}}{\left[\sum_{i=1}^{n} \left| \frac{1}{\omega_i^2} \phi_{ij}\phi_{ij} \right| \right]_{p1}} \tag{6}$$

where i is the mode number, n is the number of modes, ϕ_{ij} is the ith mode shape at jth measuring point, ω_i is the ith modal frequency.

Modal Curvature Method

Based on modal shape displacements,[33] the modal shape curvature can be approximately obtained using the central difference method as:

$$\phi''_{ij} = \frac{\phi_{i(j-1)} - 2\phi_{ij} + \phi_{i(j+1)}}{l^2} \tag{7}$$

where l is the distance between two bridge measuring points. ϕ_{ij} is ith modal shape curvature at the jth measuring point.

According to the modal curvature characteristics, the structural damage identification parameters based on the curvature of the modal shape function can be defined as:

$$MCDSI_{ij} = [\phi''_{ij}]_{p2} - [\phi''_{ij}]_{p1} \tag{8}$$

Background of Runyang Suspension Bridge

Bridge Description

Opened to traffic in 2005, the Runyang Bridge stretches across the Yangtze River, establishing a vital link between the urban regions of Yangzhou and Zhenjiang in Jiangsu Province, China. The bridge consists of a suspension bridge and a cable-stayed bridge. The Runyang suspension bridge showcases a dual-tower configuration and a three-span steel box girder design, with spans of 470, 1490, and 470 m, respectively.[34] The streamlined steel box girder boasts dimensions of 36.3 m in width and 3.0 m in height.

A comprehensive SHM system has been established to ensure the secure operation of the Runyang Suspension Bridge. This study predominantly utilizes real-time acceleration time history data captured by accelerometers on the suspension bridge's main girders. The layout of the SHM vibration system for the Runyang suspension bridge is shown in *Fig. 2*.

Complying with the requirements of modal analysis, the Runyang suspension bridge's main girder was equipped with 29 low-frequency unidirectional accelerometers strategically placed across nine cross-sections, as depicted in *Fig. 2*. Of these, 18 accelerometers monitor the main girder's vertical acceleration, and the other 11 sensors

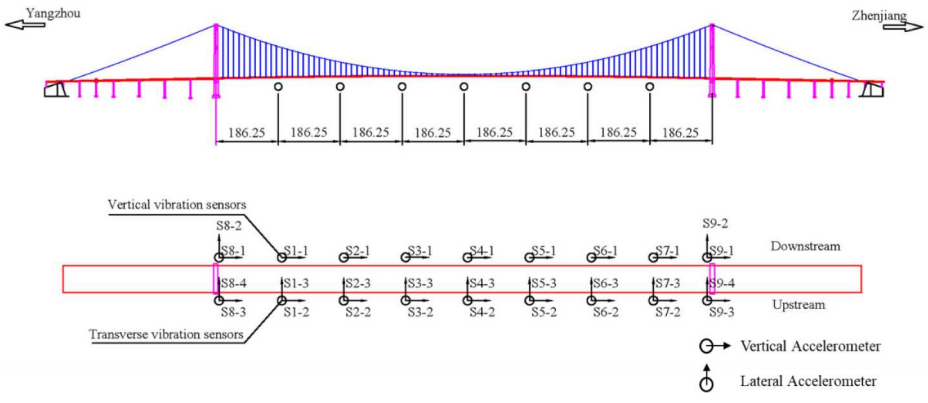

Fig. 2: Layout of accelerometers used to monitor bridge vibration. Units = m

monitor its lateral acceleration. These accelerometers operate at a sampling frequency of 20 Hz and perform continuous 24-hour real-time monitoring, generating hourly time history datasets.

The data obtained in the SHM system was extensive. Considering the computational demands and time cost, this study concentrates exclusively on the acceleration time history data derived from the left half-span of the main girder, situated near the Yangzhou side. The analysis seeks to exploit the symmetry inherent in suspension bridge design and assess the performance of the bridge under service loads.

Modal Analysis

Due to the limited number of accelerometers, only the first five vertical modes of the Runyang suspension bridge can be fully identified through the SHM vibration data. The subspace system identification (SSI) method[35] is an output-only time domain technique that directly works with time data without the need to convert them to correlations or spectra. The initial five modal parameters were obtained by operational modal analysis (OMA) using the SSI method. A comprehensive investigation of these parameters, as well as in-depth modal research on the Runyang Bridge, can be found in the references.[36,37] However, it was worth noting that the SSI modal identification did not successfully capture the 2nd mode from the SHM data. To delve into the reasons for this absence, the natural excitation technique, the eigensystem realization algorithm (NExT/ERA) method,[38] was employed for modal identification. The modal characteristics obtained from the two modal identification methods were in significant agreement, as presented in *Table 1*.

Two modal identification methods were used to determine the 2nd mode of the bridge by assessing its frequency information. Since the 2nd mode of the bridge lacks the requisite strength for identification under service loads, there was an absence of stable poles that can be recognized in the stability graph by SSI method. Furthermore, the percentage of Poles ζ was also markedly inadequate for identification in eigensystem realization algorithm (ERA) convergence studies. This observation indicated that the 2nd mode of the bridge lacked the necessary strength for identification under the service loads. Consequently, the effect of the 2nd mode would be disregarded in the subsequent analysis.

Mode	Frequency in paper[35,36] (Hz)	Frequency (Hz)		Damping (%)		Mode shape
		SSI	NExT/ERA	SSI	NExT/ERA	
VS1	0.1233	0.122	0.124	0.95	1.47	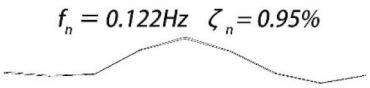
VA1	0.1441	N.A.[a]	N.A.[a]	N.A[a]	N.A[a]	N.A[a]
VS2	0.1685	0.167	0.169	0.62	2.21	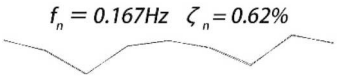
VA2	0.1880	0.187	0.188	0.59	0.76	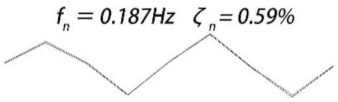
VS3	0.2402	0.237	0.238	0.21	0.235	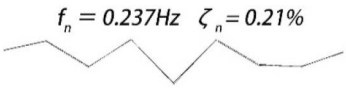

[a]SSI method missed this mode. The mode shape given by Refs. [36,37]

Table 1: Modal parameters by SSI modal identification and Refs. [36,37]

According to the modal characterization using the long-term SHM vibration data, the average mode frequencies of the bridge in 2008 were as follows: 0.12201, 0.16643, 0.18677, and 0.23827 Hz for respective modes. Over eight years of operation, the changes in modal frequencies of the Runyang Bridge were relatively small. In 2014, the corresponding average values were 0.12197, 0.16639, 0.18637, and 0.23777 Hz. The frequencies exhibit a slight reduction. Notably, the higher-order mode frequencies experienced more pronounced changes than the fundamental frequency. This variation in modal frequencies indicated that the stiffness of the Runyang Suspension Bridge transformed to a certain extent under the influence of traffic loads.

Based on the examination of the modal parameters of the bridge and the arrangement of the measuring points for structural health monitoring, the available data permitted an assessment of the first five modal parameters and corresponding mode shapes of the bridge structure. Given that the acceleration time course was sampled at 20 Hz, it was essential to focus on specific vibration frequencies in the acceleration time history and effectively capture changes in the dynamic properties of the bridge. Notably, these significant vibration frequencies were predominantly in the 0–0.3 Hz range. Then, a band-pass filter was applied as a preprocessing to capture vibrations within this frequency range while minimizing the impact of the low-frequency noise step. The original data were processed by the band-pass filter with cut-off frequencies set to 0.05 and 0.3 Hz. The first-order vibration frequency of the bridge was initially considered to be 0.122 Hz.

Damage-Sensitive Feature Analysis for Suspension Bridge by Long-Term Output SHM data

Results of Damage-Sensitive Feature Analysis

The acceleration data were obtained from five distinct measuring points on the Runyang Bridge for two time periods: January to December 2008 and January to December 2014. The acceleration time history dataset for January 2008 served as the foundational parameter values for the bridge analysis. Eqs. (2)-(5) were independently used to compute the temporal evolution of the threshold T_j for each measuring point. This variation was visually depicted in *Figs. 3–7*.

Utilizing the energy ratio Q_j at each measuring point obtained the mean value $\left(\sum Q_j\right)/n_s$of 0.2. By comparing the damage threshold value T_j with $\left(\sum Q_j\right)/n_s$, it became evident that concerning the acceleration time history

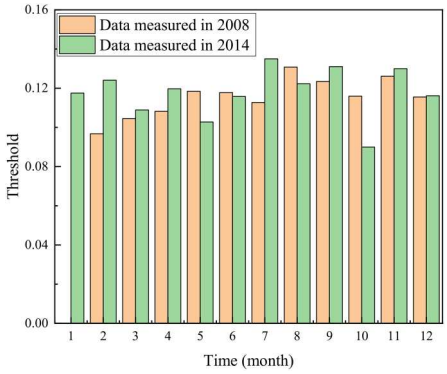

Fig. 3: Time-domain energy threshold variation at the bridge support

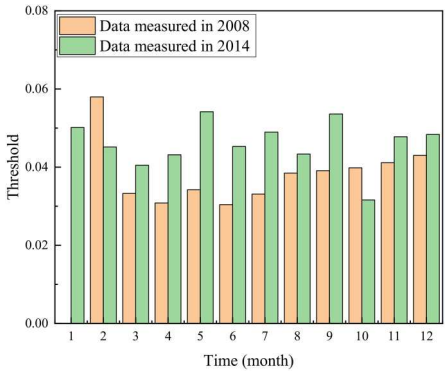

Fig. 4: Time-domain energy threshold variation at 1/8-span of the bridge

data for the Runyang Bridge in January 2008, the threshold values at each measuring point were below $(\sum Q_j)/n_s$. This observation suggested that there was no monolithic structural damage within the bridge when scrutinizing the alterations in the acceleration time-domain energy damage thresholds from 2008 to 2014, and the changes in the structure's dynamic characteristics varied considerably at different measurement points.

The changes in damage thresholds T_j for the measuring points at the bridge

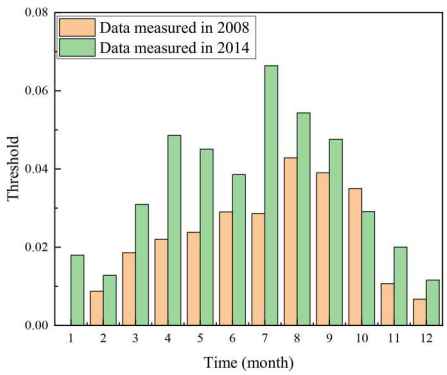

Fig. 5: Time-domain energy threshold variation at 1/4-span of the bridge

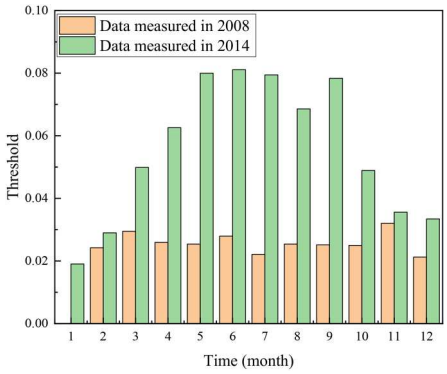

Fig. 6: Time-domain energy threshold variation at 3/8-span of the bridge

support and 1/8 span were relatively small. Comparison of the damage thresholds T_j of the measuring points at the bridge's 1/4 span and 3/8 span in 2014 with the data in 2008 indicated that the increase in T_j value at the 3/8 span exceeded the growth more than in T_j value at the 1/4 span. Furthermore, the rise in T_j value was notably more significant from March to September. For the mid-bridge location (1/2 span), the acceleration time-domain energy damage threshold T_j, for the entire year of 2014, increased significantly compared with the T_j value in 2008.

After analyzing the variation of energy damage thresholds within the acceleration time domain of the bridge based on the monitoring data, it was found that there were significant differences in the structural vulnerability of different spans of the bridge under prolonged service loads. 1/4 spans, 3/8 spans, and 1/2 spans were more susceptible to damage than bridge supports and 1/8 spans. Notably, there was a clear correlation between structural vulnerability and environmental factors such as temperature for the 1/4 and 3/8 spans.

The vibration of the bridge consisted of two main components: natural

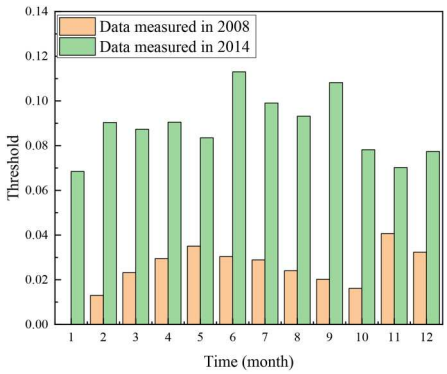

Fig. 7: Time-domain energy threshold variation at 1/2-span of the bridge

vibration (0-1 Hz) and forced vibration (2 Hz-15 Hz) induced by vehicle loading. The research result[39] indicated that the largest amplitude and power spectral density (PSD) of natural vibration under vehicle loading occurred at the 1/2 span of the bridge. Additionally, the amplitude of the PSD excited by vehicle body bounce gradually decreased from 1/8 span to 1/2 span of the bridge. However, the PSD of the bridge vibration at 1/8 span was negligible. In contrast, the 1/4 span experienced the most substantial impact due to the combined effect of forced vehicle body bouncing and the bridge's natural vibration. Therefore, the vehicle load vibration characteristics revealed that the vehicle vibration had a more pronounced effect on the bridge at 1/2 span and 1/4 span than at other locations.

Owing to the substantial spacing between the vibration measurement points along the longitudinal axis of the bridge structure, the change patterns depicted in *Figs. 3–7* appeared relatively discrete. While this permitted the assessment of bridge structure damage solely in the proximity of the measuring points under service loads, it failed to capture alteration trends in the longitudinal stiffness across the bridge.

Verification of Damage-Sensitive Feature Analysis

Fatigue crack investigation[40] of suspension bridge shows that the typical fatigue position of the steel box girder of Runyang suspension bridge is 1/4 cross-section of the girder in the longitudinal direction. The layout diagram of the typical fatigue position and vulnerable identification area by the time-domain energy method is shown in *Fig. 8*. In *Fig. 8*, the vulnerable area obtained by the time-domain energy method is located between the typical fatigue areas of the Runyang Suspension Bridge. The boundaries of the vulnerable area coincide with the typical areas of fatigue damage. Those welding fatigue cracks, which were shown in *Fig. 8*, located at the 1/4 span of the bridge would affect the stiffness of the main girder to a certain extent. At the same time, this also has a certain impact on the dynamic characteristics of the 1/4 section, 3/8 section, and 1/2 section of the main girder.

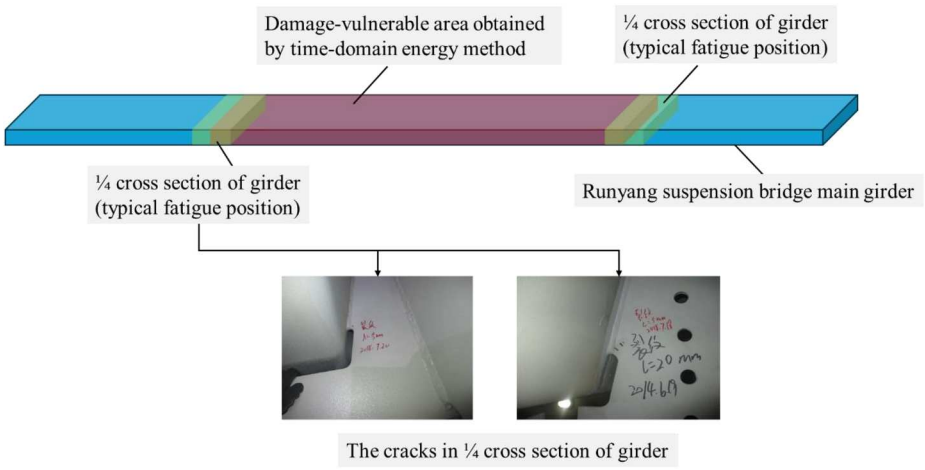

Fig. 8: The layout of typical fatigue position and vulnerable identification area by time-domain energy method

This qualitatively proves that the results obtained by the time-domain method are consistent with the fatigue disease of the Runyang Suspension Bridge.

To further demonstrate the applicability of the time-domain energy method, this study utilized the analysis results derived from vibration-based time-domain energy threshold parameters to evaluate the structural damage condition. It applied the structural modal compliance method and the structural modal curvature method.

Based on the modal methods outlined in Section 2.2 and considering the period of the Runyang Suspension Bridge SHM data, the health status of the Runyang Bridge was defined across four distinct phases: an initial phase (beginning of 2008), a one-year operation phase (end of 2008), a seven-year operation phase (beginning of 2014), and an eight-year operation phase (end of 2014). In this database, 120 data sets were selected for each analysis phase, and the outcomes were averaged after removing discrete results to ensure the precision of the damage identification.

Due to the order limitation of the modal identification of the Runyang Bridge structure, the identification errors of different damage identification methods are different. Therefore, this article uses two damage identification parameters, MFDSI and MCDSI, to verify the analysis results of the time-domain energy method. Due to the changes in modal characters, the two modal identification methods have different application scopes. The modal flexibility method has a broader scope of application. The MFDI method could be utilized to estimate the magnitude of damage in a noisy environment. However, the MSEDI could not damage the location in the presence of noise due to its high sensitivity to changes in modal data. This technique also utilizes numerical methods to calculate modal curvature, which makes it more susceptible to errors.

Based on the index of the initial stage as the reference, the MFDSI and MCDSI for the other three stages can be calculated, as illustrated in *Fig. 9* and *Fig. 10*. After one year of service, the changes of the MFDSI of the Runyang bridge shown in *Fig. 9* were primarily centered between the 1/8-span and 1/2-span. However, in *Fig. 10*, the changes in modal curvature at 1/8-span and bridge support were relatively small. In this timeframe, the changes in modal shape were predominantly localized between 1/4-span and 1/2-span, especially in the 1/2-span region.

After seven years of operation, the MFDSI and MCDSI of the Runyang Bridge exhibited further changes. Additional increases in MFDSI values were observed at the 1/8 span, 3/8 span, and 1/2 span, characterized by more pronounced peaks observed primarily at the 1/8 span and 3/8 span. In addition, the fluctuations in MCDSI also increased to some extent. Positive peaks became prominent at the 3/8-span, while negative peaks emerged at the 1/4-span and 1/2-span. These observations underscore substantial fluctuations in the modal curvature at these different positions.

Alterations in the overall stiffness parameters of the bridge can be characterized by changes in the modal flexibility index and the modal curvature index. Through this interrelation, abrupt oscillations emerged in the 1/2 and 3/8 span during the bridge's different periods, demonstrating a higher sensitivity to structural stiffness changes under prolonged service loads. In contrast, the 1/4-span of the bridge was slightly less sensitive to changes in structural stiffness than the 1/2-span and 3/8-span of the bridge.

Notably, the MFDSI values of Runyang suspension bridge distort at 1/4 and 1/2 cross section. This is consistent with the change in stiffness of the bridge main girder. The welding fatigue cracks concentrated at the 1/4 span and the central buckle at the 1/2 span, affecting the overall stiffness of the bridge and causing the MFDSI to have an inflection point at those locations. The MFDSI is relatively sensitive to the stiffness changes of the bridge. Compared with the MFDSI coefficient, the MCDSI intuitively reflects the change in the main girder's stiffness through the change in the modal curvature. The modal curvature increases significantly from 1/4, indicating that the main girder's stiffness has changed to a certain extent from 1/4 span, consistent with the damage-vulnerable area obtained by the time-domain method analysis. This also indirectly verifies

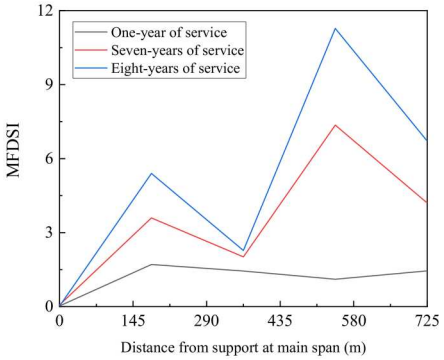

Fig. 9: MFDSI of Runyang suspension bridge

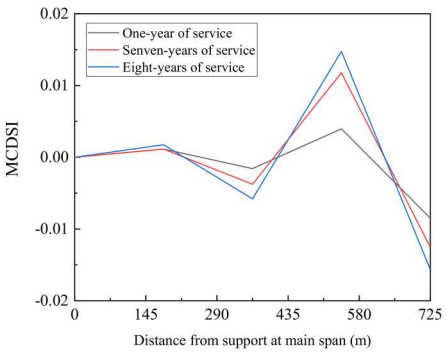

Fig. 10: MCDSI of Runyang suspension bridge

the applicability of the time-domain energy method.

Conclusions

The damage identification methods based on short-term structural performance have been extensively studied in SHM. However, there is limited research on damage identification for the long-term dynamic response of bridges. The present study used the acceleration time history of multiple measuring points on bridge girders in 2008 and 2014 for bridge damage identification through the improved time-domain energy method. On this basis, the following conclusions can be drawn:

1. The time-domain energy method performs well in identifying vulnerable areas of a suspension bridge from its long-term health monitoring data. The damaged-vulnerable area identification of the bridge girder in this study showed time-variant deterioration, leading to an elevation in the time-domain energy threshold. Significant increases of time-domain energy index were observed at the 1/4, 3/8, and 1/2 cross section of main girder. This reflects the impact of mass welding fatigue cracks distributed at the 1/4 cross-section of the main girder's steel deck. The 1/4 cross-section of the main beam with more fatigue cracks is more significantly affected by temperature. This phenomenon can more intuitively and quantitatively determine where mass fatigue cracks are distributed in the damaged-vulnerable area of the structure.
2. The structural vulnerability assessment results based on the long-term SHM data of steel box girders show that the time-domain energy method performs best among the three damage-sensitive area identification methods in this paper. The time-domain energy method can quantitatively identify the vulnerable area of the bridge and determine the bridge cross sections where mass welding fatigue cracks have appeared; MFDSI can only be used to quantitatively determine the sections where more welding fatigue cracks have appeared in steel box girder bridges; and MCDSI can only qualitatively determine the vulnerable parts of the structure.
3. This article did not consider the structural time-domain energy at higher-order natural frequencies due to the limited number of measuring points in the SHM system. Although the high-order mode vibrations accounted for a small percentage of the acceleration time history, their effects on structural damage were still not fully comprehended. When dealing with a limited number of measurement points, the impact of higher-order patterns should be further investigated.

Acknowledgment

I would like to thank you, Yaner. You let me know what it feels like to admire someone. You will listen to my complaints and comfort me when I feel confused. You taught me a lot of strange knowledge. This experience is so funny. I am fortunate to meet you. I hope you can live a smooth life in the future. We are good friends for life.

Disclosure Statement

No potential conflict of interest was reported by the author(s).

Funding

This work was supported by National Natural Science Foundation of China: [grant no 52178119]; Natural Science Foundation of China [Grant No. 51908191]; Jiangsu Provincial Transportation Technology and Achievement Transformation Project under Grant: [grant no 2022Y20].

Data Availability Statement

Due to the nature of the research, supporting data is not available.

References

[1] Shi Z, Zhou Y, Sun Z, et al. Fatigue performance of orthotropic steel decks in a wide steel-box girder. J Constr Steel Res. 2022; 190: 107109.

[2] Zhu Z, Xiang Z. Fatigue cracking investigation on diaphragm cutout in a self-anchored suspension bridge with orthotropic steel deck. Struct Infrastruct Eng. 2019; 15(10): 1279–1291.

[3] Liu J, Lu Z, Yu M. Damage identification of non-classically damped shear building by sensitivity analysis of complex modal parameter. J Sound Vib. 2019; 438: 457–475.

[4] Ling Y, Mahadevan S. Integration of structural health monitoring and fatigue damage prognosis. Mech Syst Signal Process. 2012; 28: 89–104.

[5] Capecchi D, Ciambella J, Pau A, et al. Damage identification in a parabolic arch by means of natural frequencies, modal shapes and curvatures. Meccanica. 2016; 51: 2847–2859.

[6] Ren W-X, De Roeck G. Structural damage identification using modal data. I: simulation verification. J Struct Eng. 2002; 128(1): 87–95.

[7] Ren W-X, De Roeck G. Structural damage identification using modal data. II: test verification. J Struct Eng. 2002; 128(1): 96–104.

[8] Duvnjak I, Damjanović D, Bartolac M, et al. Mode shape-based damage detection method (MSDI): Experimental validation. Appl Sci. 2021; 11(10): 4589.

[9] Feng D, Feng MQ. Output-only damage detection using vehicle-induced displacement response and mode shape curvature index. Struct Control Health Monit. 2016; 23(8): 1088–1107.

[10] Khiem NT, Tran HT. A procedure for multiple crack identification in beam-like structures from natural vibration mode. J Vib Control. 2014; 20(9): 1417–1427.

[11] Ay AM, Khoo S, Wang Y. Probability distribution of decay rate: a statistical time-domain damping parameter for structural damage identification. Struct Health Monit. 2019; 18(1): 66–86.

[12] Mustafa S, Matsumoto Y, Yamaguchi H. Vibration-based health monitoring of an existing truss bridge using energy-based damping evaluation. J Bridge Eng. 2018; 23(1): 04017114.

[13] Shahsavari V, Chouinard L, Bastien J. Wavelet-based analysis of mode shapes for statistical detection and localization of damage in beams using likelihood ratio test. Eng Struct. 2017; 132: 494–507.

[14] Aied H, González A, Cantero D. Identification of sudden stiffness changes in the acceleration response of a bridge to moving loads using ensemble empirical mode decomposition. Mech Syst Signal Process. 2016; 66: 314–338.

[15] Bai R, Radzieński M, Cao M, et al. Non-baseline identification of delamination in plates using wavelet-aided fractal analysis of two-dimensional mode shapes. J Intell Mater Syst Struct. 2015; 26(17): 2338–2350.

[16] Yuen KV, Huang K. Identifiability-enhanced Bayesian frequency-domain substructure identification. Comput-Aided Civ Infrastruct Eng. 2018; 33(9): 800–812.

[17] Günaydin M, Sunca F, Altunişik AC, et al. Nondestructive experimental measurement, model updating, and fatigue life assessment of Çarşamba suspension bridge. J Bridge Eng. 2022; 27(2): 05021017.

[18] Günaydin M, Adanur S, Altunişik A, et al. Dynamic characteristics monitoring changes of damaged and retrofitted RC buildings. Exp Tech; 2022: 1–28.

[19] Genç AF, Kahya V, Altunışık AC, et al. Assessment of modal characteristics of cross-laminated timber beams subject to successive damages. Arch Civ Mech Eng. 2021; 21(3): 128.

[20] Patel B, Dewangan U. Damage detection techniques to identify the unknown damage parameters from the structural response data in

beam: A review. Recent Trends in Civil Engineering: Select Proceedings of ICRTICE 2019. 2021: 175–183.

[21] Tefera B, Zekaria A, Gebre A. Challenges in applying vibration-based damage detection to highway bridge structures. Asian J Civ Eng. 2023: 1–20.

[22] Altunışık AC, Okur FY, Kahya V. Modal parameter identification and vibration based damage detection of a multiple cracked cantilever beam. Eng Fail Anal. 2017; 79: 154–170.

[23] Hearn G, Testa RB. Modal analysis for damage detection in structures. J Struct Eng. 1991; 117(10): 3042–3063.

[24] Nick H, Aziminejad A. Vibration-based damage identification in steel girder bridges using artificial neural network under noisy conditions. J Nondestr Eval. 2021; 40: 1–22.

[25] Farrar CR, Lieven NA. Damage prognosis: the future of structural health monitoring. Phil Trans R Soc A Math Phys Eng Sci. 2007; 365(1851): 623–632.

[26] Tibaduiza Burgos DA, Gomez Vargas RC, Pedraza C, et al. Damage identification in structural health monitoring: a brief review from its implementation to the use of data-driven applications. Sensors. 2020; 20(3): 733.

[27] Hou R, Xia Y. Review on the new development of vibration-based damage identification for civil engineering structures: 2010–2019. J Sound Vib. 2021; 491: 115741.

[28] Le NT, Thambiratnam D, Nguyen A, et al. A new method for locating and quantifying damage in beams from static deflection changes. Eng Struct. 2019; 180: 779–792.

[29] Nguyen K-D, Chan TH, Thambiratnam DP. Structural damage identification based on change in geometric modal strain energy–eigenvalue ratio. Smart Mater Struct. 2016; 25(7): 075032.

[30] Rucevskis S, Janeliukstis R, Akishin P, et al. Mode shape-based damage detection in plate structure without baseline data. Struct Control Health Monit. 2016; 23(9): 1180–1193.

[31] Fan W, Qiao P. Vibration-based damage identification methods: a review and comparative study. Struct Health Monit. 2011; 10(1): 83–111.

[32] Pandey A, Biswas M. Damage detection in structures using changes in flexibility. J Sound Vib. 1994; 169(1): 3–17.

[33] Nick H, Aziminejad A. Vibration-Based Damage Identification in Steel Girder Bridges Using Artificial Neural Network Under Noisy Conditions. J Nondestr Eval. 2021; 40(1): 1–22.

[34] Wang H, Li A, Hu R. Comparison of ambient vibration response of the Runyang suspension bridge under skew winds with time-domain numerical predictions. J Bridge Eng. 2011; 16(4): 513–526.

[35] Van Overschee P, De Moor B. A unifying theorem for three subspace system identification algorithms. Automatica (Oxf). 1995; 31(12): 1853–1864.

[36] Li Z, Li A, Zhang J. Effect of boundary conditions on modal parameters of the Run Yang Suspension Bridge. Smart Struct. Syst. 2010; 6(8): 905–920.

[37] Li Z, Feng MQ, Luo L, et al. Statistical analysis of modal parameters of a suspension bridge based on Bayesian spectral density approach and SHM data. Mech Syst Signal Process. 2018; 98: 352–367.

[38] Juang J-N, Pappa RS. An eigensystem realization algorithm for modal parameter identification and model reduction. J Guid Control Dyn. 1985; 8(5): 620–627.

[39] Shao Y, Miao C, Brownjohn J, et al. Vehicle-bridge interaction system for long-span suspension bridge under random traffic distribution. Structures. 2022; 44: 1070–1080.

[40] Zhongqiu F, Bohai J, Kunkun L, et al. Research on the Typical Fatigue Position of Steel Box Girder Suspension Bridge with Twin Towers. Highway. 2015; 60(10): 88–93.